Journal of Food Engineering 399 (2025) 112615

Contents lists available at ScienceDirect

Journal of Food Engineering

journal homepage: www.elsevier.com/locate/jfoodeng

Enhancing the processability and mechanical performance of collagen-based biofilms through supercritical carbon dioxide plasticisation

Karina C. Núñez C. [a,b,*], Luis E. Alonso Pastor [a,1], Félix Lizalde-Arroyo [a,b], Jaime Lledó [a,b], Leandra Oliveira Salmazo [a,b], Alberto Lopez-Gil [c], Miguel A. Rodríguez-Pérez [a,b]

[a] Cellular Materials Laboratory (CellMat), Condensed Matter Physics Department, Faculty of Science, University of Valladolid, Paseo de Belén, 7, 47011, Valladolid, Spain
[b] BioEcoUVA Research Institute on Bioeconomy, University of Valladolid, Spain
[c] CellMat Technologies S.L, C. del Argón, 1, 47012, Valladolid, Spain

ARTICLE INFO

Keywords:
Collagen
Supercritical carbon dioxide
Plasticisation
Biofilms
Packaging

ABSTRACT

The hierarchical structure and high molecular weight of bovine collagen fibres, along with their widespread availability, make this animal protein a promising candidate for biofilm production. However, unlike conventional thermoplastics, collagen processing is challenging due to its complex intra- and intermolecular interactions. This study investigated the use of supercritical carbon dioxide (sCO_2) as a plasticising agent to modify these interactions during a pretreatment phase prior to film formation via extrusion-compression moulding. Different supercritical conditions were tested, and the combined effect of sCO_2 and glycerol (Gly), a common plasticiser, was evaluated. Microstructural analyses of the pretreated powders and resulting biofilms revealed an unconventional plasticisation mechanism, characterised by the loss of the triple-helix structure and the formation of a randomly cross-linked network. This effect was particularly pronounced under supercritical conditions at higher temperatures (80 °C and 80–300 bar), where the loss of surface water from the collagen fibres and interactions between functional groups in denatured fibres led to enhanced plasticity. As a result, the extruded films exhibited a reduction in stiffness of up to 20 % and an increase in elongation at break by more than 50 %. In contrast, pretreatments at lower temperatures and pressures (35 °C and 80 bar) caused only minor chain scission, preserving the triple-helix structure and yielding rigid films with limited deformability. These findings demonstrated that controlling supercritical conditions in the presence of glycerol during collagen pretreatment is an effective strategy to enhance the processability and mechanical performance of collagen-based biofilms.

1. Introduction

In recent years, there has been a significant increase in interest in researching and developing more sustainable and environmentally friendly materials, particularly in the packaging industry, which is one of the largest contributors to waste generation (Fogt Jacobsen et al., 2022). This sector has led to a massive accumulation of plastics in the environment due to its linear economy model, characterised by the rapid use and disposal of products. In the context of various scientific studies, bio-based materials are considered to be at the forefront of the transition towards a more circular and sustainable economy in this sector (Mendes and Pedersen, 2021; Tardy et al., 2022; Versino et al., 2023). Understanding the origin, nature, and availability of bio-based raw materials is crucial to efficiently harness their value in achieving this transition.

In this regard, research in biomaterials for packaging is extensive (Asgher et al., 2020; Attaran et al., 2017; Sid et al., 2021). Various bio-based raw materials have been used in the preparation of food packaging films, such as microbial-origin biopolymers (e.g., PHA) (Meereboer et al., 2020), wood-based polymers (cellulose, hemicellulose, starch, and lignin) (Miranda et al., 2015; C. Zhang et al., 2020) and protein-based polymers (e.g., plant-based such as zein, gluten, soybean, etc., or animal-based such as whey, casein, gelatine, keratin, etc., and

* Corresponding author. Cellular Materials Laboratory (CellMat), Condensed Matter Physics Department, Faculty of Science, University of Valladolid, Paseo de Belén, 7, 47011, Valladolid, Spain.
E-mail address: karinacarla.nunez@uva.es (K.C. Núñez C.).
[1] Current address: Department of Manufacturing Process Engineering, School of Industrial Engineering, University of Valladolid, Paseo del Cauce, 59, 47011, Valladolid, Spain.

https://doi.org/10.1016/j.jfoodeng.2025.112615
Received 26 November 2024; Received in revised form 1 April 2025; Accepted 13 April 2025
Available online 19 April 2025

their combinations) (Calva-Estrada et al., 2019; Martins et al., 2021; R. Zhang et al., 2024). All these studies shared a common focus: investigating the plasticisation and cross-linking of bio-based chains, with particular attention to the required functionality, such as improving moisture and gas barrier properties, extending food shelf life, and, crucially, reducing environmental impact.

Gelatine, a significant collagen derivative obtained through physical, chemical, or biochemical denaturation and hydrolysis of collagen triple helix (Gorgieva and Kokol, 2011), has proven to be a valuable material in the production of biodegradable and edible films and coatings due to its excellent film-forming properties, easy availability, low cost, and biodegradability (Luo et al., 2022; Ramos et al., 2016). However, gelatine films are composed of low molecular weight peptide chains that have lost their folding and triple-helix conformation due to the breaking of their covalent bonds and their strong secondary interactions. This results in high water solubility and poor mechanical properties, limiting their use in durable, non-edible packaging applications. Significant research has been conducted to improve the properties of these films, including the use of bio-additives (Martucci et al., 2015; Stejskal et al., 2020), cross-linking (Lin et al., 2019; Martucci et al., 2012), polymer blends (Dong et al., 2023) and nanotechnology (Riaz et al., 2020; Shankar et al., 2019). Nevertheless, the gelatine films studied are generally produced by non-commercial methods such as dissolution or casting, and it is important to note that their application in the packaging industry directly competes with their current extensive use in the food and pharmaceutical industries (Alipal et al., 2021).

In response to these limitations, the use of collagen in a more native state, with a lower degree of hydrolysis (Coll), could offer significant advantages. Unlike gelatin, collagen largely retains its quaternary structure, consisting of highly oriented fibres with a high molecular weight. This structural integrity may enhance the mechanical properties of films produced from collagen, presenting a viable alternative to conventional polymers used in packaging, such as polyolefins. However, processing this type of collagen as a conventional thermoplastic (i.e., via conventional extrusion processes) presents significant challenges due to strong inter- and intramolecular interactions that restrict mobility. Under heat and shear, during processing, Coll chains tend to degrade or undergo partial cross-linking before adequate moulding is achieved (Klüver and Meyer, 2013). Consequently, some degree of prior hydrolysis is necessary. In cases where the preservation of the primary conformation is desired, complex chemical processes are required during moulding (Oechsle et al., 2016).

The hypothesis of this study was to use supercritical carbon dioxide (sCO_2) as a plasticising agent to enhance the extrusion and moulding of Coll films. Under supercritical conditions, CO_2 exhibits properties between those of a gas and a liquid, allowing it to penetrate the peptide chains of Coll fibres. This interaction alters intermolecular and intramolecular forces, increasing molecular mobility and reducing viscosity, thereby facilitating the plasticisation process.

This hypothesis is supported by the studies presented in Table 1, where the technique has been applied to various fossil-based polymers, leading to a significant reduction in their glass transition temperature (Tg) and consequently improving their flexibility and processability. Furthermore, Table 1 highlights that, over the past five years, the use of lubricants such as glycerol remains a topic of interest in polymer plasticisation research, including in protein-based materials.

Although sCO_2 has been applied to Coll fibres for various purposes, none of them is used in film manufacturing. For example, sCO_2 was used to remove excess cross-linking agents like glutaraldehyde, where studies reported a 95 % removal of impurities with minimal impact on the physicochemical properties of Coll when sCO_2 is used at 20 MPa and 37 °C (Casali et al., 2018), in bioelectronics, sCO_2 (100 bar, 40 °C) has been successfully used to remove free amino acids from porcine Coll, enhancing its electro-optic performance when used as a dielectric layer in capacitors (Huang et al., 2022). Additionally, sCO_2 has been applied in the sterilization of Coll sponges and membranes used in medical devices and tissue engineering (20 MPa, 35 °C), proving to be a better alternative to γ-irradiation sterilization (Meyer et al., 2015). In cartilage tissue engineering, CO_2 has been utilized to create Coll hydrogels as scaffolds (25 °C, 50 bar) (Fernandes-Silva et al., 2013), and as a medium for transforming hydrolysed Coll into a drug carrier material, such as lycopene, where drug impregnation was achieved at 100–140 bar and 40–50 °C (Aredo et al., 2022). In the above-mentioned studies, the authors employed mild supercritical CO_2 conditions to achieve their specific objectives, minimising any potential impact on the proteins microstructure. This approach aligns with the current state of research, as no studies to date have thoroughly investigated such effects.

The present study provides the first comprehensive investigation into the use of supercritical CO_2 as a plasticising agent to improve both the processability and mechanical properties of collagen-based films. Supercritical CO_2 was selected for its ability to modify inter- and intramolecular interactions within collagen fibres, facilitating thermoplastic

Table 1
Summary of plasticisation conditions and key results for various polymers using supercritical co_2 and glycerol as a plasticiser.

Plasticising system	Polymer	Plasticisation conditions	Main results	Ref.
Supercritical CO_2	Polystyrene	1–4 % wt. de CO_2 in extrusion process (188–220 °C and 5–30 MPa).	An effect of CO_2 plasticisation on the viscosity of the polymer was found.	Lee et al. (1999)
	Poly(L-lactic acid) Polycarbonate Polysulfone Polyphenylsulfone Polyetherimide Polyethylene Polyamide 6	150 °C, 5–25 MPa and 0.5–2 h inside of a pressure vessel.	Plasticisation of engineering polymers by lowering their T_g.	Watanabe et al. (2020)
Glycerol	Cellulose acetate	1.8, 3.6, 5.4 and 7.2 M concentration of glycerol + cellulose.	Optimal light protection and low plasticiser exudation.	Teixeira et al. (2021)
	Chitosan	10, 30 and 50 % of glycerol (w/w%) with respect to chitosan mass for solvent casting preparation.	Enhanced hydrophobicity, lower brittleness and higher T_g for cellular growth.	Caroni et al. (2021)
	Thermoplastic starch	Urea + glycerol as plasticizers in different proportions. In Extrusion and granulation process.	Urea + glycerol is more effective for plasticisation than only glycerol. Prevents starch retrogradation.	Paluch et al. (2022)
	Poly(lactic) acid	Synthesis of organic carbonates from glycerol and diethyl carbonates. Plasticisation under N_2 atmosphere.	Strain at break improvement. Tensile strength slightly reduced.	Seo et al. (2024)
	Cellulose	Solvent casting of cellulose dissolved in trifluoracetic acid + variable amounts of glycerol (up to 30–50 % wt. %).	Films evolved from rigid to ductile. Improved oxygen permeability and grease resistance.	Benitez et al. (2024)
	Soy protein isolate	Injection moulding of SPI + 30–45 wt % of different plasticizers.	Improved deformability and transparency.	Aguilar et al. (2020)

extrusion. Additionally, glycerol was incorporated as a conventional plasticiser to explore potential synergies between both plasticisation strategies. The chosen glycerol concentration was based on the most optimised proportion for polymers plasticisation, as demonstrated in Table 1. Meanwhile, the supercritical conditions were systematically varied, ranging from mild to severe, with two intermediate states designed to differentiate the effects of pressure and temperature. This study also examined the microstructural evolution of collagen throughout the different processing stages—sCO_2 pretreatment, extrusion, and compression moulding—and evaluates the mechanical and thermal properties of the resulting biofilms. Finally, the results provided insight into the plasticisation mechanism induced by this approach and its influence on the final properties of the films.

2. Materials and methods

2.1. Materials

Collagen powder (Coll) 100 % bovine called KAPRO B95 was supplied by DCP-Industry (purity >95 %, w/w) and glycerol (99 %) E−422 (Gly) supplied by Quimidroga S.A. The water used was always distilled and deionized.

2.2. Methods

The methodology followed is outlined in Fig. 1, serving as a visual guide to help readers follow the sequence of experiments and characterisations performed.

2.2.1. Pre-treatment: swelling of Coll powders in sCO_2

Collagen (Coll) powders were introduced into a reactor (pressure vessel model PARR 4681 provided by Parr Instrument Company) for 1 h under the sCO_2 conditions described in Table 2 (See setup in Fig. 2 (a)). Four distinct pre-treatments were selected: a mild condition (Cond. A: 35 °C - 80 bar), two moderate conditions (one low temperature/high pressure and one high temperature/low pressure., Cond. B: 35 °C - 300 bar and Cond. C: 80 °C - 80 bar, respectively), and a severe condition (Cond. D: 80 °C - 300 bar). These conditions were selected to comprehensively explore the effects of supercritical CO_2 while ensuring the structural integrity of collagen was preserved. Given that the minimum conditions for achieving the supercritical state are 31.1 °C and 73.8 bar and considering that collagen fibres begin to denature and degrade at temperatures above 80 °C (Miles and Bailey, 1999), an upper temperature limit of 80 °C was set to maintain their stability. Consequently, the selected temperature range for the supercritical treatments was between 35 °C and 80 °C. For pressure, values within the commonly used range for supercritical CO_2 applications were chosen, between 100 and 300 bar. The highest pressure of 300 bar was selected based on previous studies that have demonstrated successful polymer plasticisation under similar conditions (Watanabe et al., 2020). These pre-treatments were designed to differentiate the effects of pressure and temperature on the material and to establish the optimal conditions for collagen plasticisation.

Table 2
Experimental conditions for pre-treatment of collagen powders using supercritical CO_2.

Conditions		Temperature (^{0}C)	Pressure (bar)
Mild condition	**A**	35	80
Moderate conditions	**B**	35	300
	C	80	80
Severe condition	**D**	80	300

The pressure is controlled through a pressure pump model SFT-Nex10 Liquid Carbon Dioxide Pump supplied by Supercritical Fluid Technologies Inc. Additionally, a clamp heater connected to a temperature controller model CAL 3000 from West Control Solution is used to adjust the temperature of the system. Finally, an electro valve model GS048620N supplied by Parker with Kv = 1.1 L/min allows fast pressure release. The reactor was depressurised at a constant and equal rate in all cases.

Experiments were carried out in duplicate: Raw Coll (without Gly) and Coll mechanically mixed with Gly (30 wt%) at room temperature. The choice of 30 wt% glycerol was based on its widespread use in the literature as a plasticisation level for protein-based films, including collagen (Langmaier et al., 2008). This concentration ensures a balance between mechanical flexibility and structural stability, preventing brittleness at lower concentrations while minimising excessive plasticiser migration at higher levels.

The amount of Coll and Gly removed during depressurization was negligible. The collected powders were stored in sealed containers until the film fabrication and characterization process. However, for the CO_2 solubility tests, the samples were tested immediately.

2.2.2. Characterisation of sCO_2 pre-treated Coll powders

All swelling pre-treatments were repeated 10 times, and each batch was characterised separately according to the protocol defined below. Once the reproducibility of the microstructure for each batch was confirmed, the batches were combined for each condition before proceeding with the film fabrication tests.

Water solubility A portion of the CO_2 pre-treated powders was placed inside a small stainless steel mesh bag (type 316L, 50 μm pore size) to prevent particle loss while allowing water circulation and diffusion of soluble fractions. The mesh bag containing the powders was then placed in an oven at 60 °C for 24 h to dry, and the initial mass was recorded. After drying, the mesh bag with the powders was submerged in a beaker with distilled water (pH = 6, at a water/sample ratio of 450:1) and gently stirred at 23 °C for 24 h. Following this, the non-soluble residue, still contained within the mesh bag, was dried at 60 °C for 24 h in an oven under a pressure of 30 mbar. (Gómez-Estaca

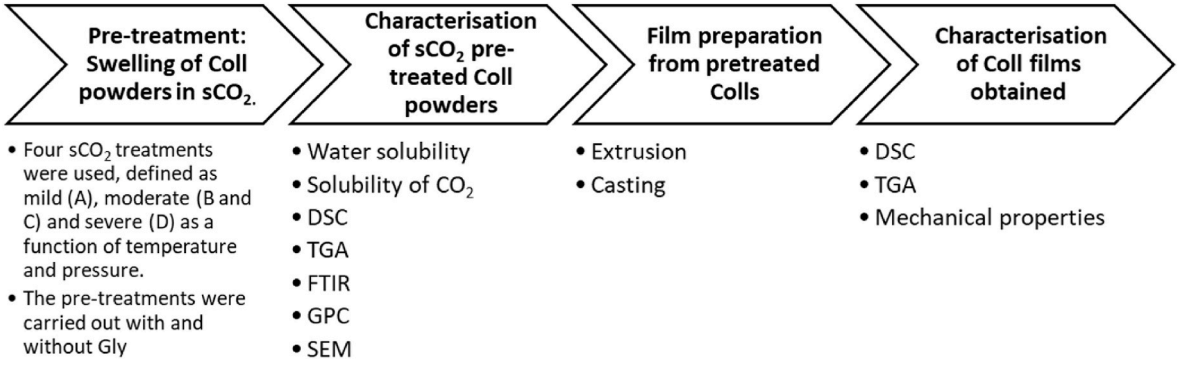

Fig. 1. Schematic representation of the methodology applied in this study, illustrating the key stages of the process.

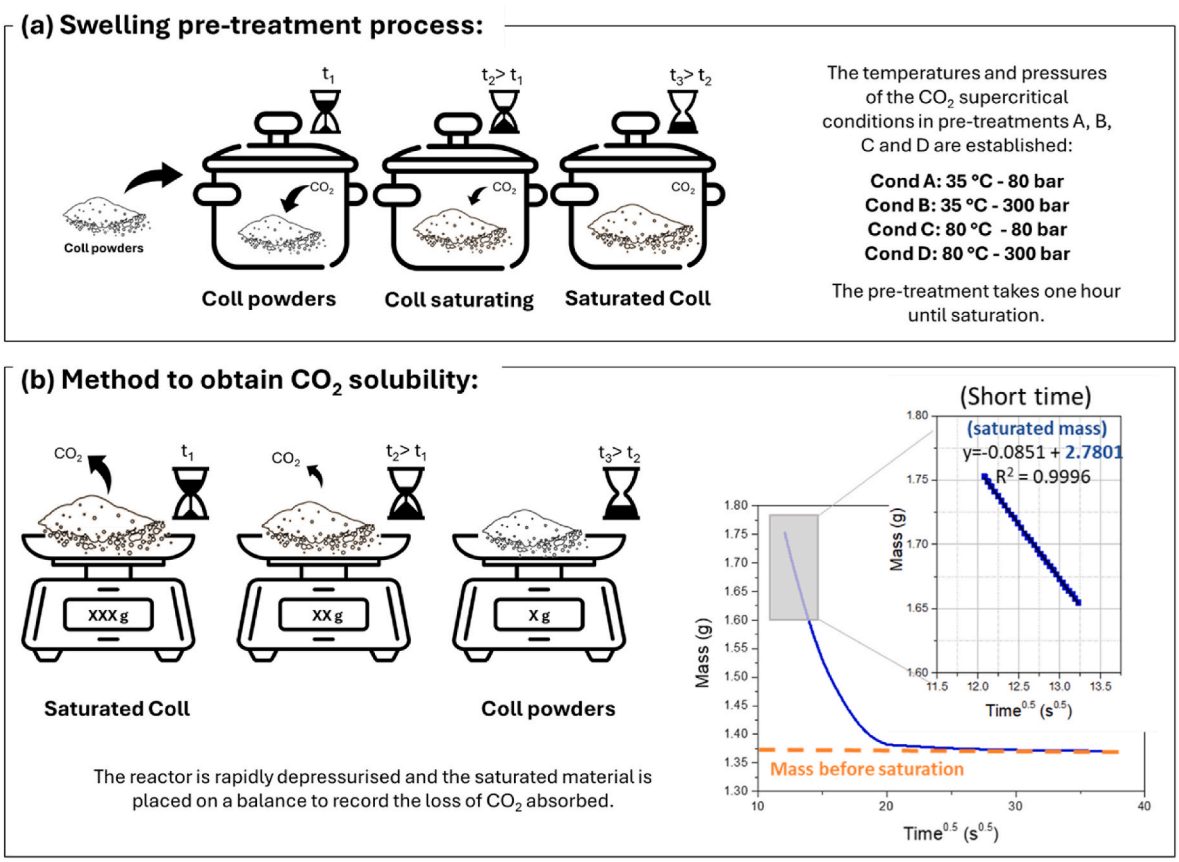

Fig. 2. (a) Swelling pre-treatment process in which CO_2 is dissolved in the material under controlled conditions of pressure and temperature. (b) Methodology for CO_2 solubility determination, in which mass loss is recorded as CO_2 is released from the sample after removal from the saturation process. An example of a desorption curve of mass vs. square root of time and zoom in on the first seconds of the desorption curve is also presented. Extrapolation of the CO_2 solubility value for time 0 s.

et al., 2009). The solubility of the powders was calculated as Equation (1.):

$$Solubility\ in\ H_2O\ (\%) = \frac{m_o - m_f}{m_o} \cdot 100 \quad (1.)$$

where, m_0 = Initial mass of the sample (including the mass of the metal mesh used to separate the soluble and insoluble fractions, which remains constant throughout the experiment), m_f = Mass of the undissolved dried powder residue (also including the mass of the metal mesh).

This water solubility measurement is inversely proportional to the % of crosslinking resulting in the collagen powders after the sCO_2 pre-treatment.

Solubility of CO_2 in collagen powders was determined from the mass increase between the initial sample and the saturated sample after the swelling process in the reactor (see Fig. 2 (b)). This method is widely used to evaluate the solubility of gases in polymeric materials, such as polymethyl methacrylate (PMMA) (Martín-de León et al., 2024) or polycarbonate (PC) (Guo & Kumar, 2015).

The mass difference between the initial sample and the saturated sample corresponds to the amount of CO_2 dissolved in the material and was quantified using an analytical balance model AT261 supplied by Mettler-Toledo (minimum detectable mass: 0.015 mg), recording the evolution of mass loss as a function of time after reactor depressurization. This process is necessary because the gas trapped in the collagen samples gradually diffuses out of the material after it is removed from the reactor in the saturation process. To estimate the saturated mass, mass loss was plotted as a function of the square root of time and fitted linearly in the initial region (see Fig. 2(b)). This estimation was used because pure collagen powders can be approximated as a collection of spheres, allowing the application of Fick's diffusion equations for spherical geometry. However, the aim of this study was to compare the CO_2 adsorption capacity of pure collagen (Raw Coll) and collagen with glycerol (Coll + Gly). Since the addition of glycerol alters the material's morphology, representing the data as a function of the square root of time provides a more suitable basis for comparing both formulations. All solubility tests were repeated 10 times per sample.

The volumetric expansion was investigated using Scanning electronic microscopy (SEM), FlexSEM 1000 VP-SEM (Hitachi High-Technologies). Samples were cryo-fractured, and the cross-sections were sputter-coated with gold before microscopic observation. The structures obtained from the collagen samples were visualized using scanning electron microscopy (SEM). A FlexSEM 1000 VP-SEM microscope at 10 kV was used for the observations, and the samples were metallized with a thin layer of gold approximately 13 nm thick using a sputter coater (model SCD 005, from Balzers Union). At least three micrographs at different magnifications and from different areas were taken for each sample.

Thermal transitions were measured using Differential Scanning Calorimetry (DSC) with a DSC model 821e thermal analysis system supplied by Mettler Toledo. The temperature range was set from 10 to 150 °C, with a heating rate of 5 °C min^{-1} under a nitrogen flow. The tests were conducted on the powders almost immediately after pre-treatment in sCO_2 and repeated after two months to assess the possible reversibility of the changes induced by sCO_2. Thermogravimetric analysis (TGA) was used to study the thermal stability of Coll powders and the amount of water and plasticiser lost in sCO_2 pre-treatment. Thermograms were obtained in a nitrogen atmosphere with a temperature sweep from 50 °C to 950 °C and a heating rate of 20 °C min^{-1} using a model TGA851e thermal analysis system supplied by Mettler Toledo. All thermal tests were repeated 10 times.

FTIR (Fourier Transform Infrared Spectroscopy) was used to monitor the changes in the secondary structures of collagen. The equipment used was a model Tensor27 spectrometer supplied by Bruker. All measurements were conducted between 600 and 4000 cm^{-1} using an attenuated total reflection (ATR) accessory equipped with a diamond ATR crystal. Each spectrum was obtained with 32 scans at a resolution of 4 cm^{-1}. At least 10 spectra were obtained from different parts of the same sample.

The molecular weight was determined using Gel Permeation Chromatography (GPC), utilizing columns specifically designed to determine molecular weights exceeding 1 million Daltons. An model 1260 HPLC system was employed for this purpose supplied by Agilent, equipped with both a refractive index detector and a dual-angle static light scattering detector. For the chromatographic separation, four columns with varying pore sizes were utilized: a Proteema precolumn (5 μm, 8 × 50 mm), Proteema 1000 Å, Proteema 300 Å, and Proteema 100 Å. Collagen samples, both Coll and Coll + Gly (with or without pre-treatment in CO_2), were dissolved in the mobile phase (3 mg/mL) and subjected to continuous stirring for 24 h to achieve optimal dissolution. The samples were then centrifuged and filtered. Subsequently, 100 μL of the filtered solution was injected for chromatographic analysis. Data analysis was conducted using the Agilent GPC/SEC A.02.01 software.

The complete dissolution of the studied samples was not possible, so only the soluble fraction was analysed using this test. In this regard, only samples A and D, both with and without glycerol, were analysed by GPC (three GPC tests were repeated for each sample). This decision was made because no significant changes were observed in their soluble fractions after treatment under moderate conditions (B and C).

2.2.3. Film preparation from pre-treated Colls

Two methods for moulding films from the pre-treated collagen samples were employed to demonstrate the potential of the technology, comparing conventional extrusion (by melt) with a laboratory-scale casting technique, which was also used to isolate the effect of mechanical stress induced by extrusion on plasticisation.

2.2.3.1. Melt. The pre-treated Colls were homogenised by melt blending in a twin-screw extruder model ZK 25 T supplied by Collins, length-to-diameter ratio (L/D) of the extruder was 24. Using temperature profile ranging from 70 °C to 90 °C, with a rotational speed of the screw of 60 rpm. If the samples did not contain the plasticiser from the sCO_2 pre-treatment, it was added during the extrusion process (30 wt %) to ensure consistency across samples and to better understand the effect of CO_2 on the incorporation of the plasticiser. After cooling, the material was pelletised using a pelletising die model SP-1 supplied by Collins. The various Coll pellets were then thermoformed into films using a model P200E hot plate hydraulic press supplied by Collins. The compression moulding process was conducted at a temperature of 80 °C and a pressure of 30 bar over 5 min.

2.2.3.2. Casting. The Coll solutions were prepared according to the traditional casting method, wherein pretreated Colls were mixed with distilled water at a ratio of 50 wt % under mechanical stirring at 70 °C for 30 min (not all samples reached solubilisation). In the same way, as in the melting process, the pre-treated Coll samples without Gly were plasticised by adding the plasticiser to the solution (30 wt %). The solutions, prepared with the same dry matter content to ensure consistent thickness, were poured onto glass Petri dishes. The solutions were dried at 30 °C in a convection oven until a constant weight was achieved.

All resulting films had a thickness of approximately 80 μm, and they were then stored at 23 ± 2 °C in a chamber with 50 ± 2 % relative humidity.

2.2.4. Characterisation of Coll films obtained by extrusion and casting process

The same DSC and TGA method used to study the thermal transitions and structural rearrangement of the pre-treated Coll powders were used for the final biofilms. The mechanical properties of the resulting biofilms were measured as follows: Young's modulus at a speed of 1 mm min^{-1} and Tensile strength was measured at a speed of 50 mm min^{-1} following the guidelines of ISO 527–1:2019, 'Plastics — Determination of tensile properties — Part 1: General principles.' At least twenty type 1A specimens were tested, and the measurements were conducted using a universal testing machine Model 5500R60025 of the Instron brand.

Statistical analysis. Data were presented as mean value ± standard deviation of realised replicates. Additionally, the Shapiro-Wilk normality test was conducted using the Python programming language (version 3.8) with the 'SciPy' library. The results of the tests demonstrated that all data obtained in the study followed a normal distribution.

3. Results

The results were presented in two parts: the first focused on the morphological changes in the protein powders after the sCO_2 pretreatment, while the second examined the mechanical characterisation of the biofilms produced from this pre-treated material, aiming to establish the relationship between the pre-treatment and the plasticisation.

3.1. sCO_2 pre-treatment: pre-moulding step

Once the Coll powders, with and without Gly, were subjected to the sCO_2 treatment described in the experimental section 2.2.1, the characterisation of the powders yielded the following results:

Solubility tests. Two important parameters can be crucial in describing the plasticising effect of sCO_2 on the collagen structure: its solubility in water and its ability to absorb CO_2 into its structure.

The change in water solubility may indicate an increase or loss of molecular weight, which is related to molecular mobility. Native collagen is insoluble in water due to its fibrillar structure, but when subjected to hydrolysis (either enzymatic or acidic), the bonds that maintain this structure are broken, forming smaller collagen peptides that can interact with water. These soluble collagens have been the most studied in film formation (Tang et al., 2022). The collagen used in this research has a water solubility of around 50 wt %, indicating that it is partially hydrolysed. In the case of CO_2 solubility in collagen, it is used as a measure to describe the interactions between the gas and the CO_2-philic chemical groups within the protein, as a means of overcoming the strong secondary interactions that limit its movement. Gas sorption in macromolecular chains results in an increase in free volume and the mobility of polymer segments, acting as a "lubricant" (Kikic et al., 2003). To study these two aspects, solubilisation tests were designed in four conditions (A, B, C, and D) were selected (see Experimental Section).

Fig. 3 presents the results for water solubility (shown as lines on the left) and CO_2 solubility (shown as bars on the right), divided into two populations: those without Gly (unshaded area, above) and those containing Gly (shaded area, below). Additionally, both tests are represented as a function of temperature (T) and pressure (P) to clearly illustrate the individual effects of each parameter on the measured properties.

The following important observations can be seen from the results depicted in Fig. 3.

1. In the samples without Gly (unshaded area), the water solubility results show that changing from a mild to a moderate pre-treatment in sCO_2 (e.g., from Cond. A to Cond. C (increased temperature) or from Cond. A to Cond. B (increased pressure), see blue lines in Fig. 3) can lead to an increase in solubility of approximately 10 % and 20 %,

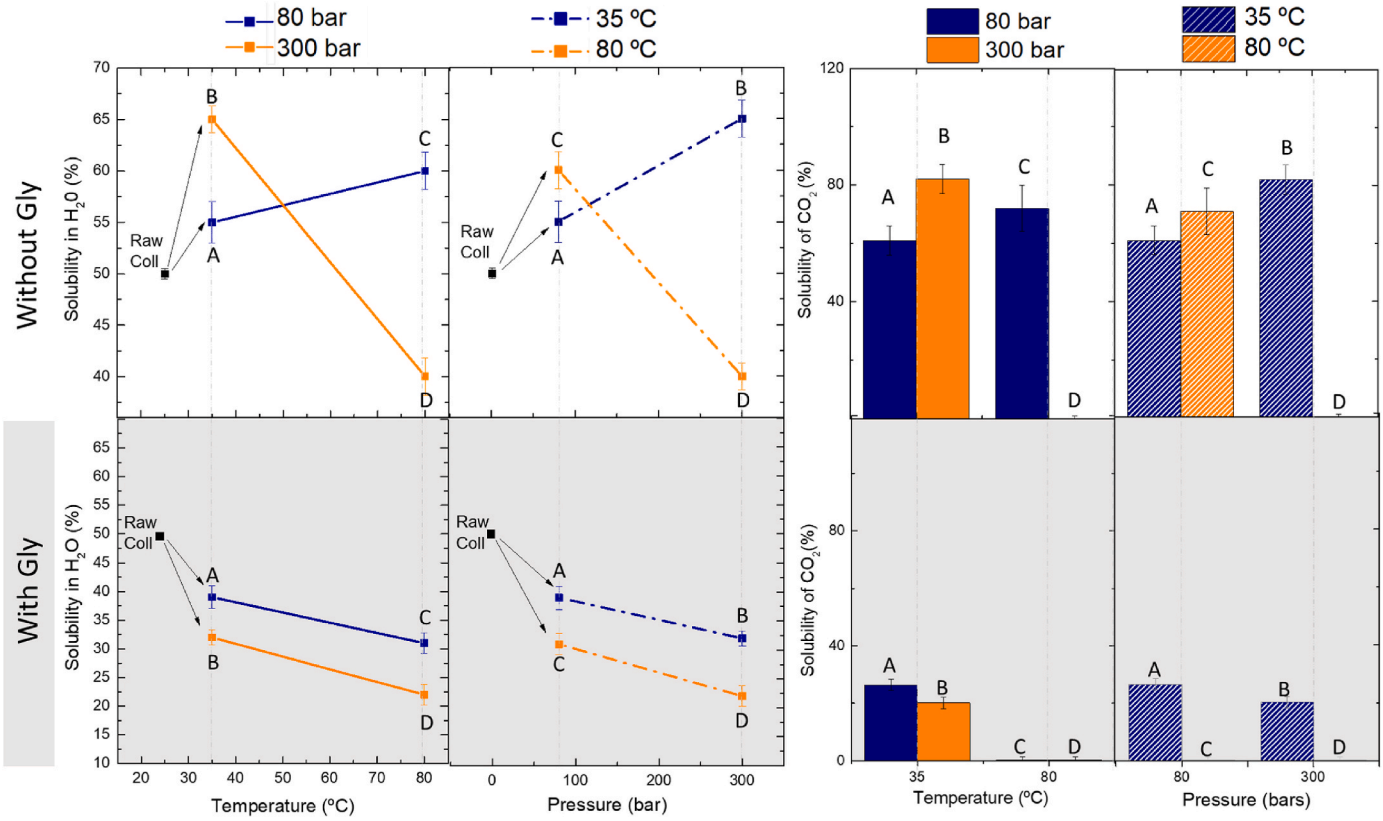

Fig. 3. Water solubility tests (lines on the left) and solubility of CO_2 in Coll (bars on the right), for samples with Gly (unshaded area, top) and without Gly (shaded area, bottom). The same results are presented as a function of temperature and pressure.

respectively. Pressure appears to be the most significant factor, as indicated by the steeper slope. This behaviour is completely reversed when the change occurs from a moderate to a severe pre-treatment (e.g., when comparing Cond. B and Cond. D (temperature change) or Cond. C and Cond. D (pressure change)), where the samples lose approximately 25 % of their water solubility in either case. Additionally, there appears to be a directly proportional relationship between water solubility and CO_2 absorption capacity. The more soluble the sample is in water, the greater the amount of CO_2 it can absorb (see when comparing the change from mild conditions (A) to moderate conditions (B or C), blue line in Fig. 3), and the less soluble the sample is, the less CO_2 it can absorb (see when comparing the change from medium conditions (B or C) to severe conditions (D), orange line in Fig. 3).

2. All samples containing a plasticiser (shaded area) exhibit a significant loss of water solubility, which appears to be more pronounced under the most severe treatment (nearly 60 % loss of water solubility when comparing the untreated collagen sample with the one treated under Cond. D, see Fig. 3). Additionally, compared to the samples without a plasticiser, they have drastically lost their ability to absorb CO_2, particularly when pre-treated at higher temperatures (Cond. C and D).

In the present study, the sCO_2 treatments aimed to enhance its absorption to disrupt secondary interactions between collagen fibres and improve plasticisation. The results suggest that a mild to moderate pre-treatment in sCO_2 can facilitate greater CO_2 absorption, provided no plasticiser is present. Interestingly, the use of a plasticiser appears to induce a form of cross-linking that reduces both water solubility and CO_2 absorption. In light of these findings, the following sections discuss the microstructural changes induced by these treatments in collagen, how they influence the observed results, and the underlying plasticisation mechanism when using sCO_2 and glycerol as a plasticiser.

GPC. When the GPC results were analysed (see Table 3 and Fig. 4), it was observed that the two extreme conditions studied, Cond. A (mild) and Cond. D (severe), in both samples with and without glycerol, showed significant changes in the molecular weights of their soluble fraction, which explains the previous observations. The intermediate conditions (Cond. B and Cond. C), as they did not show significant

Table 3
Molecular weight measurements of the soluble fraction of raw collagen samples and collagen samples subjected to pre-treatments a and d, with and without glycerol, using GPC analysis and its standard deviation.

Sample		Peak	Molecular weight (kDa)[a]
Raw Coll		1	–
		2	456 ± 42
		3	84 ± 6
		4	–
Without Gly	**A**	1	321 ± 21
		2	108 ± 7
		3	87 ± 11
		4	33 ± 4
	D	1	721 ± 38
		2	217 ± 14
		3	167 ± 6
		4	–
With Gly	**A**	1	628 ± 44
		2	306 ± 26
		3	184 ± 18
		4	–
	D	1	–
		2	155 ± 19
		3	–
		4	–

[a] Three samples were analysed for each material type, and the standard deviation of these measurements is reported.

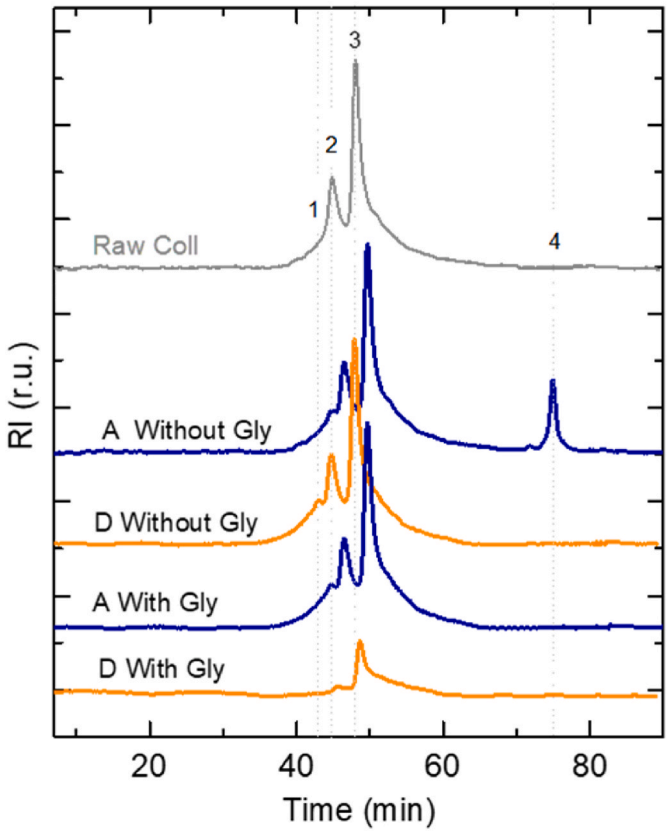

Fig. 4. GPC curves representing the different molecular weight distributions of the soluble portion for the two extreme conditions studied (Cond. A and D), with and without glycerol, compared to untreated pure collagen.

changes in water solubility, were not analysed by GPC. Instead, the study focused on the most divergent conditions.

In this regard, subjecting pure collagen fibres, without a plasticiser, to mild supercritical conditions (Cond. A) resulted in breakage of the protein fibres, causing the peaks in the GPC curves to shift, and a lower molecular weight peak is observed (see peak 4 in Fig. 4), which explains the increase in water solubility. However, when without Gly fibres are subjected to more severe conditions (Cond. D), the GPC signals shift to lower retention times, indicating the presence of fractions with higher molecular weights. This suggested the occurrence of chain cross-linking, which was responsible for the loss of solubility in water under these conditions. In the case of samples with plasticiser, regardless of the supercritical conditions, cross-linking always occurred; indeed, the sample with pre-treatment D with Gly had practically lost all of its soluble fraction.

With molecular weight being the factor that determines water solubility, it would be important to understand the mechanisms driving these changes during collagen pretreatment in CO_2 with and without glycerol. In this regard, the results of Casali and collaborators (Casali et al., 2018) suggested in their studies on the purification of collagen fibres that under sCO_2 conditions (20 MPa and 37 °C), there may be a decrease in pH due to the combined presence of carbon dioxide and the structural water of collagen at saturation pressures, which forms carbonic acid (see Equation (2)).

$$CO_2 + H_2O \longrightarrow H_2CO_3 \rightleftharpoons HCO_3^- + H_3O^+$$

Numerous studies demonstrate the crucial importance of adjusting pH in collagen formulations, as it significantly affects the stability of the triple helix and, consequently, its solubility. The effect of pH on collagen films is primarily related to the isoelectric point of the protein (Branderburg et al., 1993). The isoelectric point of collagens similar to those used in this study typically falls between 6 and 7.5. When collagen is far from its isoelectric point, the repulsive forces within the molecule increase, causing the molecular chain to stretch and exposing the internal groups on the surface (T. Zhang et al., 2022). Particularly at low pH levels (2.5–5.0) in bovine collagen fibres, soluble collagen trimers tend to form into disorganised molecular aggregates and dissociate into poorly formed their solubility (Harris and Reiber, 2007). However, as the pH rises, the exposed disulfide bonds and thiol groups react with each other, ultimately leading to an increase in the degree of cross-linking (Hellauer and Winkler, 1975; Mauri and Añón, 2006).

Thus, this could explain the behaviour of the pre-treated samples in sCO_2. On one hand, in pre-treatment A (35 °C–80 bars), the intrinsic water absorbed by collagen in a compressed liquid state acidifies the medium and causes breakage of the fibres (increased water solubility, see Fig. 3). On the other hand, in pre-treatment D (80 °C–300 bar), the samples lost almost all surface water, as demonstrated by the TGA tests (described later), and simultaneously exhibited a significant reduction in water solubility (suggesting cross-linking, see Fig. 3). However, water loss alone does not necessarily imply that it is the cause of cross-linking. Rather, the increased molecular mobility in the presence of the plasticiser could have facilitated interactions between reactive groups on the collagen fibres, leading to the formation of a cross-linked network, as evidenced by the FTIR analyses presented later. This, in turn, may have reduced the ability of the collagen to reabsorb water, which remains in a compressed liquid state under these pre-treatment conditions.

Interestingly, Miles et al. (2005) demonstrated that collagen cross-linking induces dehydration by reducing intermolecular spacing, thereby decreasing intrafibrillar water content and increasing thermal stability. Although our study does not directly examine the same mechanisms, our findings align with the idea that a cross-linked collagen structure retains less water. In this context, the surface water loss observed in pre-treatment D could be a consequence of the cross-linking process.

However, it is important to note that the denaturation temperature of the protein is reported to be between 40 and 50 °C (Hellauer and Winkler, 1975; Miles and Bailey, 1999) therefore, as the supercritical conditions become more severe, particularly in terms of temperature, there is greater mobility that exposes nearby reactive groups, enhancing cross-linking—especially if the plasticiser is present, as the results have demonstrated.

DSC. Table 4 and Fig. 5 present the results of the analysis of the endotherms from the DSC tests. The dotted lines in Fig. 5 (a) and (b) represent the same test repeated after the samples had been stored for two months to determine whether the changes in conformation were reversible.

Several observations can be drawn from these results. Firstly, in all sCO_2 pre-treatments of Coll samples without Gly (Fig. 5 (a)), no signal of a glass transition temperature (Tg) is observed, nor is there a significant change in the shape of the endotherm (indicating that the high conformational hierarchy of the triple helix is maintained). However, the enthalpies, or the area under the curve, and the peak temperatures of the endotherms have changed slightly (See Table 4). As the pre-treatment becomes more severe, the peak temperatures increase, and the enthalpies decrease. These results confirm the solubility findings, suggesting that cross-linking is promoted, but within a more disordered structure.

A bimodal denaturation process for collagen in nitrogen has generally been described in DSC tests: an initial endotherm at lower temperatures signals the disassembly of supramolecular complexes (i.e., the separation of different collagen molecules from one another), and a larger second endotherm indicates the unfolding of each individual triple-helical collagen molecule into a random coil formation (Staicu et al., 2015). As can be seen in the samples without Gly (Fig. 5 (a)), only the second denaturation mechanism is possible, meaning a rearrangement into a more disordered conformation occurs. This type of

Table 4
Enthalpy values, peak endothermic temperature (t_{max}), and glass transition temperature (Tg) of the studied collagen powders (a) with glycerol and (b) without glycerol, measured by DSC analysis with standard deviations.

Samples	(a) Without Gly[a]		(b) With Gly[a]		
	Enthalpy (J/g)	T_{max} (°C)	Tg (°C)	Enthalpy (J/g)	T_{max} (°C)
Coll	72.21 ± 1.43	83.31 ± 1.60	54.10 ± 2.16	13.72 ± 0.62	88.75 ± 1.89
A	65.63 ± 1.82	82.55 ± 1.23	52.58 ± 2.36	25.12 ± 0.26	85.58 ± 2.25
B	67.26 ± 1.38	82.48 ± 1.88	51.22 ± 1.82	22.30 ± 0.55	81.17 ± 2.28
C	60.80 ± 1.37	87.46 ± 1.43	54.85 ± 2.65	9.12 ± 0.29	86.18 ± 1.59
D	56.65 ± 1.56	91.06 ± 1.34	50.97 ± 1.87	9.77 ± 0.19	84.85 ± 1.87

[a] Ten samples were analysed for each material type, and the standard deviation of these measurements is reported.

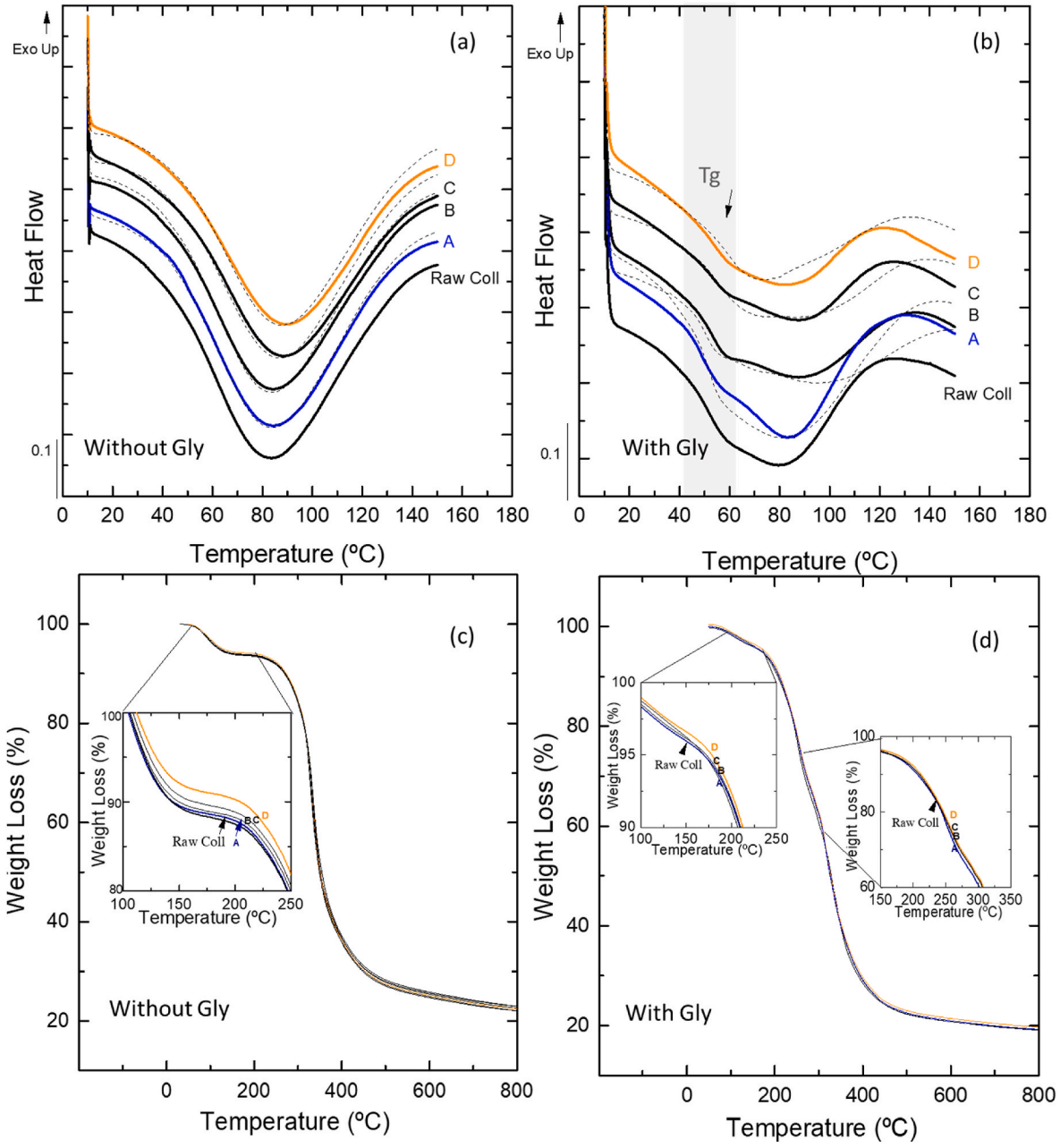

Fig. 5. Thermal transition curves for collagen powders pretreated in sCO_2: (a) DSC curves for samples without glycerol, (b) DSC curves for samples with glycerol, (c) TGA curves for samples without glycerol, highlighting changes in surface water loss, and (d) TGA curves for samples with glycerol, showing the absence of surface water and a consistent glycerol content across all samples.

denaturation requires a lower peak temperature in samples with lower molecular weight (Cond. A) and a higher temperature in those with cross-linking (Cond. D), as expected.

The completely opposite behaviour is observed in the pre-treated samples with a plasticiser (see Fig. 5 (b)). In all cases, a type of glass transition is clearly noticeable around 50 °C, which indicates a molecular transition that confers greater mobility or plasticisation. Additionally, a very broad endotherm with two merged peaks can be seen, indicating that, in this case, both previously mentioned denaturation mechanisms are occurring. It is remarkable that this substantial enthalpy loss, potentially associated with the formation of a new cross-linked structure, was compatible with a material exhibiting a pronounced glass transition, suggesting increased molecular mobility.

Finally, after two months of storage, the DSC tests were repeated, revealing that the changes were largely maintained over time. Any minor variations observed could be attributed to the increased molecular mobility conferred by glycerol and its natural exudation process over time (see Fig. 5 (b)).

TGA. Thermogravimetric analysis has allowed for the confirmation of the sample composition and their thermal stability, providing further support for the previous results. The decomposition of the samples occurs in four main steps: Step 1 corresponds to the free water in the collagen structure (boiling around 90 °C) and it represents a key indicator for monitoring the amount of surface water in collagen after each treatment and its potential influence on the plasticisation process.; Step 2 corresponds to the evaporation of the plasticiser, in the case of samples containing it (around 255 °C); Step 3 corresponds to the decomposition of the protein (around 335 °C); and finally, there is an inorganic fraction residue that does not decompose before 815 °C.

Table 5 and Fig. 5 (c) and (d) present the residue values at the corresponding decomposition temperatures for each case. Firstly, the samples without glycerol, as expected, do not show any plasticiser weight loss, while the samples with glycerol appear to have a fairly homogeneous composition, with approximately 30 wt % of plasticizers. This demonstrates that there was no significant loss of plasticiser during the applied procedures. On the other hand, the samples without glycerol subjected to mild conditions (i.e. Cond. A) retain the largest amount of water present in the collagen structure, supporting the hypothesis of medium acidification when CO_2 and water are present, leading to the potential chain scissions observed in the GPC tests.

As discussed in previous sections, the fraction of surface water decreases in collagen samples after pre-treatment under conditions C and D, meaning that water does not play a determining role in the plasticisation process under these conditions. Additionally, an increase in thermal stability is observed, as the protein decomposition temperature rises from 331 °C in Condition A to 342 °C in Condition D, representing an increase of over 10 °C in thermal stability (see Table 5). This is consistent with other cross-linking evidence, such as reduced water solubility, and with the findings of Miles et al. (2005) who establish a relationship between thermal stability and the water content in cross-linked collagens. Furthermore, the most cross-linked samples (those pre-treated with Gly) exhibit the highest decomposition temperatures, supporting the formation of a new interlinked structure under these conditions.

Finally, it is noteworthy that the samples pre-treated with glycerol generally exhibit a lower capacity to absorb water compared to their glycerol-free counterparts (see Fig. 5(c) and (d)). It is important to remember that glycerol acts as a plasticiser by interacting with amino, carboxyl, and hydroxyl functional groups, forming hydrogen bonds (Maria Martelli et al., 2006). Additionally, glycerol is quite hydrophilic, which would typically suggest that samples with Gly would have a greater capacity to absorb water. However, the overall results obtained demonstrate that, in sCO_2, plasticiser does not function in conventional form; instead, it promotes cross-linking, thereby reducing the availability of functional groups in collagen for water absorption.

FTIR. These studies confirmed the availability of functional groups in collagen to interact with glycerol, CO_2, or to form cross-links following the applied pre-treatments. Fig. 6 (a) presents the curves for all the samples studied, along with the quantitative analysis of the characteristic Amide A peak at approximately 3300 cm^{-1}, which corresponds to the stretching vibration of the N-H bond in conjunction with the O-H bond (see Fig. 6 (b)). Additionally, the ratio of (AIII/A1450) is displayed in Fig. 6 (c).

The most noticeable aspect of Fig. 6 (a) is that the samples containing glycerol exhibit a greater area under the Amide A bands compared to their glycerol-free counterparts, regardless of the applied pre-treatment. Furthermore, as the conditions in supercritical CO_2 become more severe, the Amide A peak shifts to lower wavelengths and displays a reduced area under the curve (regardless of whether the sample contains glycerine, see Fig. 6 (b)). This suggests that the -NH and -OH groups are strongly involved in the morphological changes described thus far.

In general, the monitoring of the plasticisation of collagen fibres involves tracking the change in the characteristic Amide A peak as an indication of the presence of hydrogen bonds between collagen chains. A decrease in this peak signifies the disruption of protein-protein interactions, as demonstrated by Albuquerque et al. (2020). Interestingly, the samples exhibiting a greater area are those containing the plasticiser; thus, in conjunction with previous results, it can be established that glycerol, in the presence of supercritical CO_2, does not function as a conventional plasticiser. On the contrary, these chain-chain interactions are more pronounced due to the crosslinking that has already been indicated in the earlier results.

However, when only the samples containing glycerol are examined, an increase in pre-treatment severity results in a decrease in absorbance and area (see Fig. 6 (b)), which is incompatible with the crosslinking signals presented in the earlier tests. This phenomenon may be

Table 5
Weight loss percentages for the thermal transitions of studied collagen samples: step 1 (surface water loss), step 2 (glycerol evaporation), step 3 (protein degradation), and step 4 (inorganic residue), measured through TGA analysis with its standard deviations.

Samples	Without Gly[a]				With Gly[a]			
	Step 1 (%)	Step 2 (%)	Step 3 (%)	Step 4 (%)	Step 1 (%)	Step 2 (%)	Step 3 (%)	Step 4 (%)
Coll	12.1 ± 0.6 (91 °C)	–	72.7 ± 1.5 (334 °C)	17.0 ± 1.0 (815 °C)	2.1 ± 0.2 (92 °C)	33.1 ± 2.6 (256 °C)	48.7 ± 1.6 (340 °C)	15.0 ± 1.3 (815 °C)
A	9.0 ± 0.3 (88 °C)	–	70.7 ± 2.4 (331 °C)	17.1 ± 0.8 (815 °C)	3.0 ± 0.1 (101 °C)	31.4 ± 2.0 (254 °C)	45.5 ± 2.1 (345 °C)	11.1 ± 1.8 (815 °C)
B	6.1 ± 0.2 (89 °C)	–	71.0 ± 1.3 (329 °C)	17.0 ± 1.5 (815 °C)		32.9 ± 1.6 (254 °C)	47.8 ± 2.0 (348 °C)	12.0 ± 1.1 (815 °C)
C	1.2 ± 0.2 (91 °C)	–	70.7 ± 1.2 (338 °C)	17.8 ± 1.6 (815 °C)	–	32.9 ± 1.2 (257 °C)	49.2 ± 1.8 (348 °C)	11.1 ± 1.2 (816 °C)
D	–	–	71.6 ± 1.6 (342 °C)	16.6 ± 0.9 (815 °C)	–	32.8 ± 1.7 (254 °C)	47.0 ± 1.1 (350 °C)	12.0 ± 1.3 (815 °C)

[a] Ten samples were analysed for each material type, and the standard deviation of these measurements is reported.

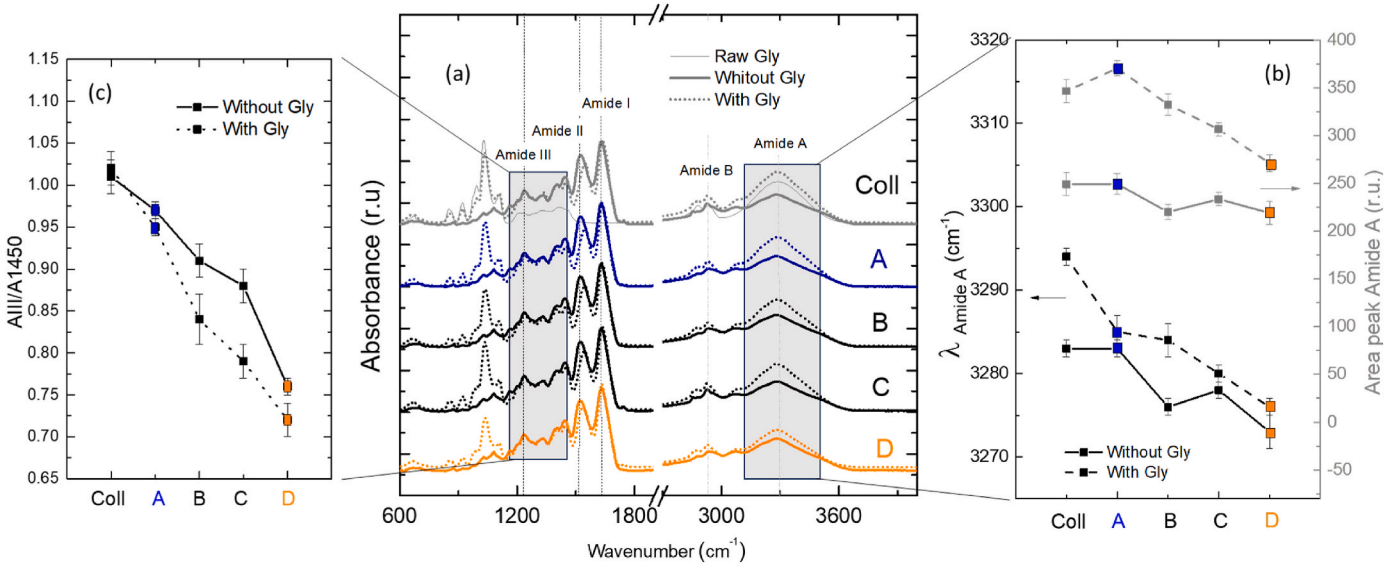

Fig. 6. (a) FTIR spectra of collagen powders pretreated with sCO_2, (b) quantitative analysis of the characteristic Amide A band to track collagen chain–chain interactions under each applied treatment, and (c) absorption ratios of AIII/A1450 to assess the stability of the triple-helix structure of collagen fibres after treatment.

explained by the physical swelling effect that supercritical CO_2 has on the protein, which expands its structure and disrupts the hydrogen bonds of Amide A, forming voids within the structure. The monitoring of the microstructure via SEM is illustrated, starting from the untreated collagen sample (Fig. 7 (a)), followed by the swollen collagen powder after pre-treatment D without glycerol (Fig. 7 (b)), and finally, the porous structure formed upon applying pre-treatment D to the collagen powder with glycerol.

sCO_2 produces a swelling effect that generates mobility within the polymer chain, which subsequently may reduce the penetration of the IR beam, resulting in less intense interactions within the collagen (Albuquerque et al., 2020). Furthermore, in more crosslinked structures, this physical foaming phenomenon becomes quite evident, as the molecular entanglements contribute to an enhancement of the "melt strength," promoting a stable cellular structure as the protein becomes more crosslinked (see Fig. 7 (c)), this is similar to the foaming behaviour observed in synthetic polymers (Escudero et al., 2016). This foaming effect has been found to be irreversible following depressurization; however, as will be demonstrated in the following section, it disappears when the film is produced.

Another relevant aspect of the volumetric expansion or foaming induced by sCO_2 in the presence of glycerol is the generation of significant free volume between the protein chains. This free volume could be responsible for the pronounced glass transition (Tg) observed in the DSC tests (see Fig. 5 (b)). Thus, the appearance of Tg in the thermograms could be primarily attributed to a physical effect. However, when analysing the curve for collagen with glycerol without pre-treatment, this transition can already be inferred, highlighting the crucial role of glycerol in the plasticisation process, beyond the mere swelling of the protein after the sCO_2 treatment. In this context, it is relevant to mention previous studies on the foaming of synthetic polymers, where it has been reported that the confinement of chains in cellular walls tends to limit their mobility, particularly in nanocellular structures (Martín-de León et al., 2024). Nevertheless, in this case, the protein chains appear to be in a swollen and interlinked state (with irregular cells at the micrometric scale, see Fig. 7 (c)), which, along with the plasticising effect of glycerol, results in very pronounced glass transitions.

Finally, when returning to FTIR results (Fig. 6 (a)), additional observations can be made. For instance, less significant changes are observed in the characteristic peak of Amide B at approximately 3085 cm^{-1}, attributed to the O-H stretching vibration, as well as in the symmetric and asymmetric stretching vibrations of aliphatic -CH groups in $-CH_3$ and $-CH_2$, respectively, near 2852 cm^{-1}. However, in pre-treatment D, both with and without glycerol, the absorbance and area tend to be lower than in the other treatments, as these groups are also involved in the formation of highly branched structures (T. Zhang et al., 2022).

Very minimal changes are also observed in the peaks of Amides I, II, and III. The first, near ~1630 cm^{-1}, corresponds to the C=O stretching vibration of the peptide bond; the second, near ~1545 cm^{-1}, is associated with the N-H bending vibration and C-N stretching vibration; and the third, near ~1236 cm^{-1}, relates to the C-N stretching and N-H bending vibrations of the amide bonds, as well as the $–CH_2$ bending vibration from the glycine and proline side chains (Sionkowska, 2004).

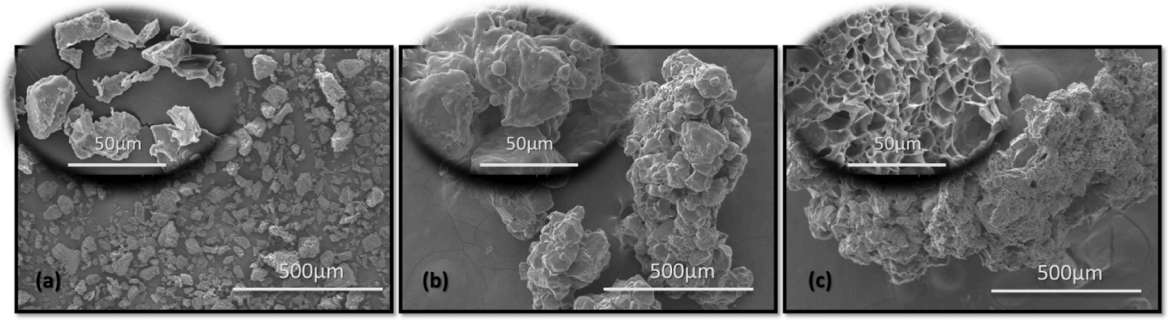

Fig. 7. Scanning electron microscopy (SEM) of collagen powders (a) Raw Coll, (b) Coll without Gly with pre-treatment D and (c) Coll with Gly with pre-treatment D.

This suggests that primarily the -OH and -NH groups (broad Amide A peak) are involved in the observed cross-linking, which appears to be random in nature.

The peak at the wavelength of 1034–1036 cm^{-1} in all samples containing plasticiser is associated with the -OH group, primarily due to glycerol (Hoque et al., 2011). This peak exhibited a smaller amplitude, and a slight band shift compared to the control raw Gly band. This indicates that the glycerol is present and not removed during pre-treatment, as confirmed by the TGA analysis, and further suggests that it interacts with the matrix.

Finally, the characteristic FTIR bands also allow for the study of the absorbance ratio (AIII/A1450), which indicates the integrity of the collagen triple helix structure. According to findings by Andrews et al. (2003) the absorbance ratio (AIII/A1450) for collagen with an intact triple helix structure is approximately 1, and this value decreases with the loss of triple helicity. The data reported in Fig. 6 (c) align with the notion that the integrity of the collagen triple helix structure in the samples decreases after treatments that induce crosslinking compared to non-crosslinked samples. This reduction could be attributed to the covalent crosslinks formed within the helix, which would disrupt the hydrogen bonds that maintain the triple helix structure.

Finally, it is demonstrated that collagen powders do not respond uniformly under all supercritical conditions. However, there is a clear trend where, as the conditions become more severe and in the presence of a plasticiser, a type of interconnected random coil structure tends to form.

3.2. Evaluation of films obtained from sCO_2 pre-treated collagen: moulding step

Up to this point, it has been demonstrated that subjecting collagen powders to different conditions of sCO_2, with and without Gly, results in significant changes in the microstructure that are not entirely related to the typical concept of plasticisation: the breaking of intra- and intermolecular secondary interactions, denaturation, high CO_2 absorption, or significant increases in solubility. However, it is possible to assess the utility of these changes on the mechanical properties of films obtained from the treated collagens. In Fig. 8, Young's Modulus, Tensile Stress, and Elongation at Break measured in a unidirectional tensile test for the films obtained from pre-treated Coll at different sCO_2 conditions, with and without plasticiser are showed.

Before describing the results, it is important to emphasise, as outlined in the experimental section, that all characterised films contain glycerol in the same amount (30 wt %). The difference lies in the timing of its addition during the processing. The results presented in Fig. 8 (a) correspond to films in which the precursor powder was pre-treated with supercritical CO_2 without glycerol, the plasticiser was added during the extrusion process. In contrast, Fig. 8 (b) corresponds to the results of films where the plasticiser was incorporated during the precursor pre-treatment in sCO_2, meaning that no additional plasticiser was introduced during extrusion. The results of the TGA test confirmed this homogeneous composition (see Table 5).

The collagen film derived from untreated collagen, plasticised during extrusion, generally exhibits a stiffer behaviour (see Fig. 8). However, the significant measurement errors and the quality of the extrudate and pressed material indicate that it is not a stable, well-plasticised material. Moreover, it exudes the plasticiser within a few days, as has been observed (Sothornvit and Krochta, 2005), (see Fig. 9, where the quality of the extrudate and a lightly pressed film is observed).

Regarding the films obtained from the treated collagen powders, the various microstructural changes in collagen induced by the different conditions of supercritical CO_2 have indeed altered the mechanical behaviour of the reference material. For example, in the films obtained from the powders without glycerol during the pre-treatment in sCO_2 (Fig. 8 (a)), it is clear that the loss of molecular weight and the preservation of the hierarchical triple helix conformation in sample form Cond. A are reflected in the higher stiffness values and the lower elongation at break values. As the pre-treatment in sCO_2 becomes more severe, the previously described signs of crosslinking emerge, indicated by an increase in deformability, and in the most crosslinked sample (i.e. Cond. D), there is also an increase in tensile strength, suggesting a possible type of strain hardening. It is important to remember that the films were obtained through compression moulding; thus, unaligned films are tested, and a rearrangement of the collagen fibres can occur in the direction of the stress, thereby increasing their strength through the formation of new secondary interactions.

In the case of focusing on the samples that contained glycerol from

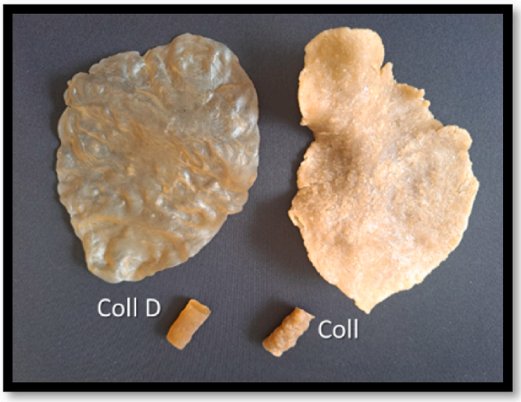

Fig. 9. Comparative between pressed extrudates obtained from untreated collagen (Coll) and collagen with pre-treatment D with glycerol (Coll D).

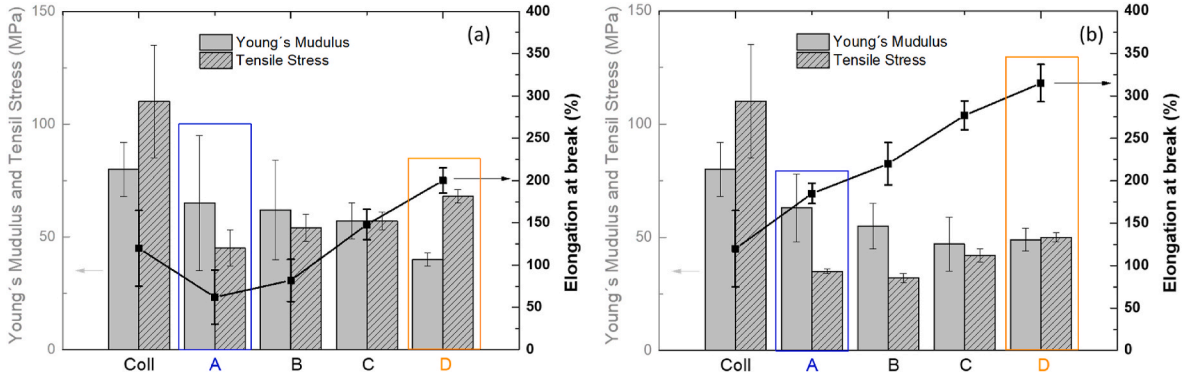

Fig. 8. Mechanical properties: Young's Mudulus, Elongation at break and Tensile stress of Collagen Film from pre-treated powders in sCO_2 (a) without glycerol and (b) with glycerol.

their pre-treatment in sCO_2 (Fig. 8 (b)), a clear increase in elongation at break can be observed across all applied treatments, in addition to lower values of modulus and tensile strength. This can be inferred from the characterization results of the powders: the pre-treatment in supercritical CO_2 and glycerol work synergistically in a type of plasticisation based on the disruption of secondary interactions, resulting in a disordered interconnected structure, indicative of a type of cross-linking. This disordered interconnected bovine conformation does not provide significant improvements in mechanical strength, as is often observed in crosslinked polymer structures. However, it contributed to considerable stability and flexibility in the film (as evidenced by the reduction in error bars).

Finally, it can be discerned whether the final mechanical properties are significantly influenced by the thermo-mechanical shear of the extrusion process or if they are solely a consequence of the microstructure of the precursor powders following pre-treatment. To investigate this, the evolution of the microstructure was compared through DSC testing for three groups of pairs: precursor powder ($Coll_p$) versus the resulting films ($Coll_f$) in Fig. 10 (a). Group I corresponds to collagen without pre-treatment, group II corresponds to collagen subjected to pre-treatment D without Gly, and the third group corresponds to collagen pre-treated with Cond. D and Gly.

In the case of the first group, it is evident that there are minimal conformational changes from the powder to the film, as has been reported (Klüver and Meyer, 2013; Oechsle et al., 2016) without a real plasticisation process due to the limited molecular movements of the triple helix. Once again, the rough product and orange peel texture of the extrudate from the reference material (Coll) can be observed in Fig. 9. In any case, the extrusion did not result in a significant change in the microstructure of the film.

In group II, the change from precursor powder to film is surprising (practically all of the area under the endotherm has disappeared, indicating the loss of the conformational hierarchy of the collagen triple helix), demonstrating that merely subjecting the protein to that pre-treatment under severe supercritical CO_2 conditions significantly enhances the thermo-mechanical effect of extrusion on the microstructure and plasticisation.

Finally, in the third group, the powder has considerably changed its microstructure compared to pure collagen powder due to the previously described synergy between the use of glycerol and supercritical CO_2 during the pre-treatment. Nevertheless, a loss of enthalpy and a broadening of the endotherm are still observed in the final film, indicating that this structure continues to evolve towards a more disordered arrangement after moulding process. Remarkably, even after extrusion, the presence of a secondary transition (Tg) remains clearly observable in this group of samples. This indicates that it is not merely a physical effect due to the foaming of the precursor, as discussed earlier, but rather that there is indeed a plasticisation in the powder structure that is retained and even enhanced during the formation of the film. This is evidenced by the decrease in Tg (see the change in the glass transition in Fig. 10 (a)), which may result from improved interaction and penetration of the plasticiser within the structure due to the sCO_2, based on how it was added.

It may be reasonable to think that the changes could be associated with alterations in the final composition of the films. However, Fig. 10 (b) demonstrates that all the films have a very similar composition, as

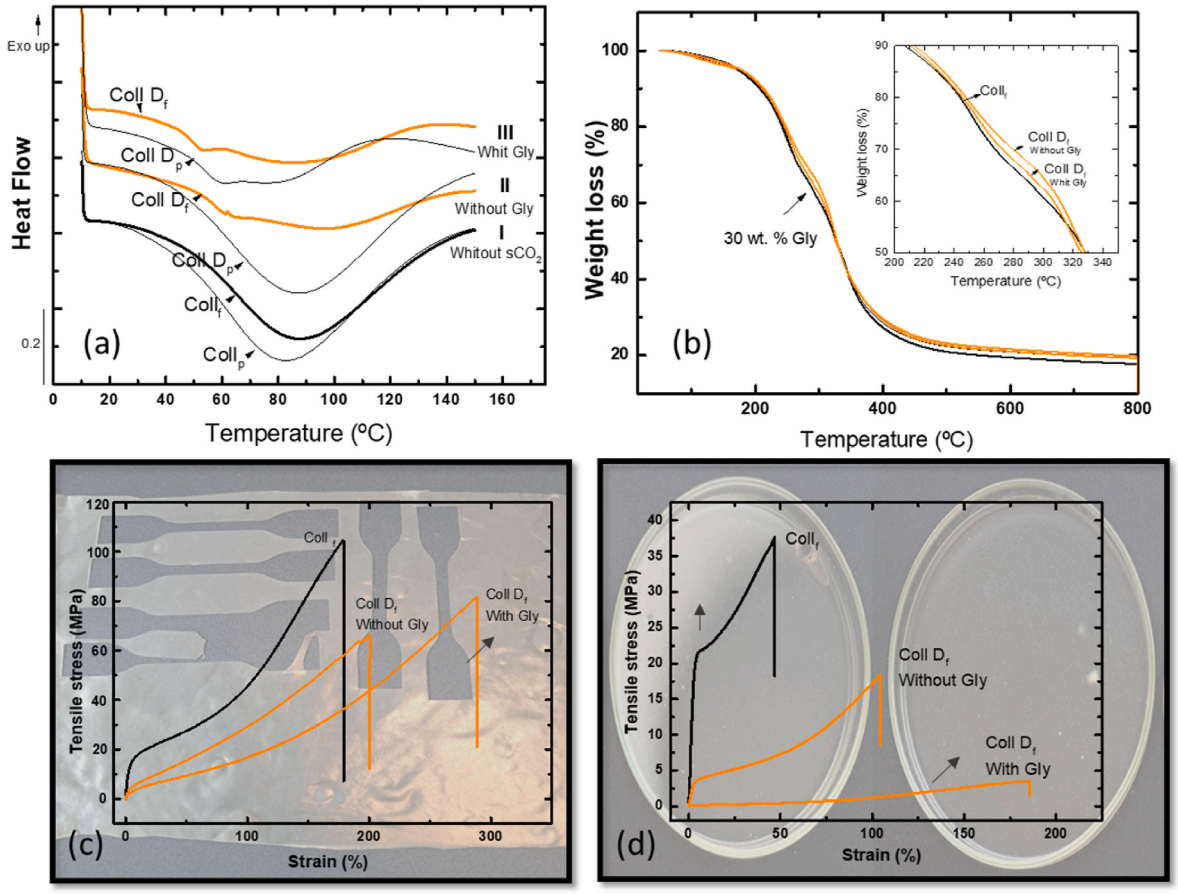

Fig. 10. (a) DSC curves for three pairs of precursor powder groups ($Coll_p$) versus their corresponding films ($Coll_f$), for samples without sCO_2 pre-treatment (I), with pre-treatment D without Gly (II) and with Gly (III), (b) TGA curves of the films analysed in (a), (c) Tensile stress-strain curve for films obtained by extrusion, with a sample of the film from Coll D with Gly shown at the bottom of the image, and (d) Tensile stress-strain curve for films obtained by casting, with a comparison of a film from raw Coll and from Coll with pre-treatment D with Gly shown at the bottom of the image.

evidenced by a decomposition step of 30 wt % of the mass occurring at around 220 °C, which is attributed to the plasticiser. Furthermore, no changes can be observed in the region corresponding to the water decomposition.

Finally, the collagen powder subjected to pre-treatment D with and without Gly was used not only to obtain films by melt extrusion (see the quality of the film, particularly Coll D with Gly at the bottom of the image, and the mechanical properties graphs in Fig. 10 (c)) but also by casting process (see the obtained films and summary of mechanical properties in Fig. 10 (d)). This demonstrates that not only the treatment in sCO_2 can enhance extrusion but also casting processes that are typically used only for soluble proteins.

Although the collagen powders subjected to pre-treatment D showed a decrease in solubility, the resulting microstructural change—characterised by a more disordered and denatured network—improves solvent penetration and swelling, which in turn facilitates the formation of cast films. This is illustrated in the image at the bottom of Fig. 10 (d): on the left, the untreated collagen is insoluble, resulting in uneven areas in the film, while on the right, a well-formed film with a smooth surface is observed, owing to the homogeneous swelling of the pre-treated collagen powder. These cast films possess mechanical properties consistent with this method of fabrication, which are not comparable to those obtained via melt extrusion (Hernandez-Izquierdo and Krochta, 2008; Ochoa-Yepes et al., 2019). However, the use of this method has allowed for a retrospective comparison between the commonly used laboratory technique for obtaining protein films and a commercial method, such as those employed in the production of thermoplastic films.

The successful formation of these films by extrusion indicates true plasticisation of the collagen powders, achieved through the adjustment of pre-treatment conditions in supercritical CO_2. This process does not lead to protein degradation but instead induces notable conformational changes, which present an interesting avenue for further study and potential applications.

4. Conclusion

The use of supercritical CO_2 for plasticising collagen-based biofilms has not been explored until now. This study presents a method to systematically investigate the influence of each step in the film production process, starting from collagen pre-treated with sCO_2, on the mechanical properties of the final biofilms. The results demonstrate that when collagen is treated under sCO_2 conditions above its denaturation temperature (80 °C, 80–300 bar), the combination of CO_2 and glycerol significantly alters its secondary structure and intermolecular interactions. This leads to a more disordered, cross-linked structure that facilitates the production of highly plasticised films. The treated collagen powders, which swell due to gas absorption and show increased molecular mobility, become more water-insoluble and perform better during extrusion, preventing issues such as melt fractures or uneven surfaces. As a result, the films produced exhibit up to 20 % less rigidity and a 50 % increase in elongation at break. These findings provide valuable insights into how more extreme supercritical CO_2 conditions affect collagen fibres compared to conventional processing methods. This knowledge extends beyond biofilm production, offering a foundation for applications where controlled conformational changes in collagen are desired, positioning supercritical CO_2 as an effective tool for modifying collagen's microstructure.

CRediT authorship contribution statement

Karina C. Núñez C.: Writing – original draft, Supervision, Methodology, Investigation, Funding acquisition, Formal analysis, Data curation, Conceptualization. **Luis E. Alonso Pastor:** Writing – review & editing, Visualization, Validation, Methodology, Data curation. **Félix Lizalde-Arroyo:** Writing – review & editing, Validation, Methodology, Data curation. **Jaime Lledó:** Writing – review & editing, Validation, Methodology, Data curation. **Leandra Oliveira Salmazo:** Writing – review & editing, Software, Formal analysis. **Alberto Lopez-Gil:** Writing – review & editing, Software, Formal analysis. **Miguel A. Rodríguez-Pérez:** Validation, Methodology, Funding acquisition, Formal analysis.

Declaration of competing interest

The authors declare the following financial interests/personal relationships which may be considered as potential competing interests: K. C.N.C. reports financial support was provided by Spain Ministry of Science and Innovation. M.A.R.P. reports financial support was provided by Government of Castile and León. If there are other authors, they declare that they have no known competing financial interests or personal relationships that could have appeared to influence the work reported in this paper.

Acknowledgement

The authors gratefully acknowledge the financial support of the "Ministerio De Ciencia E Innovación, Unión Europea.-Next Generation UE, Agencia Estatal De Investigación, Plan De Recuperación, Transformación Y Resiliencia" for the ECOLAYER project (TED2021-129419B-C22, K.C.N.C.). They also express their appreciation for the Recovery and Resilience Mechanism Funds (New Generation EU and Castilla y León Funds), under the Complementary Research and Development Plans with the Autonomous Communities in R&D&I actions, Component 17 - Investment 1 (M.A.R.P). Additionally, the authors thank the University of Valladolid for the Postdoctoral Contract awarded under the 2020 Call (K.C.N.C.).

Data availability

The data that has been used is confidential.

References

Aguilar, J.M., Bengoechea, C., Pérez, E., Guerrero, A., 2020. Effect of different polyols as plasticizers in soy based bioplastics. Ind. Crop. Prod. 153, 112522. https://doi.org/10.1016/j.indcrop.2020.112522.

Albuquerque, G.A., Bezerra, F.W.F., de Oliveira, M.S., da Costa, W.A., de Carvalho Junior, R.N., Joele, M.R.S.P., 2020. Supercritical CO_2 Impregnation of piper divaricatum essential oil in fish (Cynoscion acoupa) skin gelatin films. Food Bioprocess Technol. 13 (10), 1765–1777. https://doi.org/10.1007/s11947-020-02514-w.

Alipal, J., Mohd Pu'ad, N.A.S., Lee, T.C., Nayan, N.H.M., Sahari, N., Basri, H., Idris, M.I., Abdullah, H.Z., 2021. A review of gelatin: properties, sources, process, applications, and commercialisation. Mater. Today Proc. 42, 240–250. https://doi.org/10.1016/j.matpr.2020.12.922.

Andrews, M.E., Murali, J., Muralidharan, C., Madhulata, W., Jayakumar, R., 2003. Interaction of collagen with corilagin. Colloid Polym. Sci. 281 (8), 766–770. https://doi.org/10.1007/s00396-002-0843-4.

Aredo, V., Passalacqua, E.S., Oliveira, A. L. de, 2022. Hydrolysed collagen as carrier material for particle formation via supercritical CO_2 impregnation. J. Supercrit. Fluids 188, 105647. https://doi.org/10.1016/j.supflu.2022.105647.

Asgher, M., Qamar, S.A., Bilal, M., Iqbal, H.M.N., 2020. Bio-based active food packaging materials: sustainable alternative to conventional petrochemical-based packaging materials. Food Res. Int. 137, 109625. https://doi.org/10.1016/j.foodres.2020.109625.

Attaran, S.A., Hassan, A., Wahit, M.U., 2017. Materials for food packaging applications based on bio-based polymer nanocomposites. J. Thermoplast. Compos. Mater. 30 (2), 143–173. https://doi.org/10.1177/0892705715588801.

Benitez, J.J., Florido-Moreno, P., Porras-Vázquez, J.M., Tedeschi, G., Athanassiou, A., Heredia-Guerrero, J.A., Guzman-Puyol, S., 2024. Transparent, plasticized cellulose-glycerol bioplastics for food packaging applications. Int. J. Biol. Macromol. 273, 132956. https://doi.org/10.1016/j.ijbiomac.2024.132956.

Branderburg, A.H., Weller, C.L., Testin, R.F., 1993. Edible films and coatings from soy protein. J. Food Sci. 58 (5), 1086–1089. https://doi.org/10.1111/j.1365-2621.1993.tb06120.x.

Calva-Estrada, S.J., Jiménez-Fernández, M., Lugo-Cervantes, E., 2019. Protein-based films: advances in the development of biomaterials applicable to food packaging. Food Eng. Rev. 11 (2), 78–92. https://doi.org/10.1007/s12393-019-09189-w.

Caroni, J.G., de Almeida Mattos, A.V., Fernandes, K.R., Balogh, D.T., Renno, A.C.M., Okura, M.H., Malpass, A.C.G., Ferraresi, C., Garcia, L.A., Sanfelice, R.C., Pavinatto, A., 2021. Chitosan-based glycerol-plasticized membranes: bactericidal and fibroblast cellular growth properties. Polym. Bull. 78 (8), 4297–4312. https://doi.org/10.1007/s00289-020-03310-4.

Casali, D.M., Yost, M.J., Matthews, M.A., 2018. Eliminating glutaraldehyde from crosslinked collagen films using supercritical CO 2. J. Biomed. Mater. Res. 106 (1), 86–94. https://doi.org/10.1002/jbm.a.36209.

Dong, Y., Rao, Z., Liu, Y., Zheng, X., Tang, K., Liu, J., 2023. Soluble soybean polysaccharide/gelatin active edible films incorporated with curcumin for oil packaging. Food Packag. Shelf Life 35, 101039. https://doi.org/10.1016/j.fpsl.2023.101039.

Escudero, J., Lopez-Gil, A., Laguna-Gutierrez, E., Rodriguez-Perez, M.A., 2016. Low density non-crosslinked closed/open cell polypropylene foams with high mechanical properties. Cell. Polym. 35 (3), 101–118. https://doi.org/10.1177/026248931603500301.

Fernandes-Silva, S., Moreira-Silva, J., Silva, T.H., Perez-Martin, R.I., Sotelo, C.G., Mano, J.F., Duarte, A.R.C., Reis, R.L., 2013. Porous hydrogels from shark skin collagen crosslinked under dense carbon dioxide atmosphere. Macromol. Biosci. 13 (11), 1621–1631. https://doi.org/10.1002/mabi.201300228.

Fogt Jacobsen, L., Pedersen, S., Thøgersen, J., 2022. Drivers of and barriers to consumers' plastic packaging waste avoidance and recycling – a systematic literature review. Waste Manag. 141, 63–78. https://doi.org/10.1016/j.wasman.2022.01.021.

Gómez-Estaca, J., Montero, P., Fernández-Martín, F., Gómez-Guillén, M.C., 2009. Physico chemical and film-forming properties of bovine hide and tuna skin gelatin: a comparative study. J. Food Eng. 90 (4), 480–486. https://doi.org/10.1016/j.jfoodeng.2008.07.022.

Gorgieva, S., Kokol, V., 2011. Collagen- vs. gelatine-based biomaterials and their biocompatibility: review and perspectives. In: *Biomaterials Applications for Nanomedicine*. InTech. https://doi.org/10.5772/24118.

Guo, H., Kumar, V., 2015. Some thermodynamic and kinetic low-temperature properties of the PC-CO2 system and morphological characteristics of solid-state PC nanofoams produced with liquid CO_2. Polymer 56, 46–56. https://doi.org/10.1016/j.polymer.2014.09.061.

Harris, J.R., Reiber, A., 2007. Influence of saline and pH on collagen type I fibrillogenesis in vitro: Fibril polymorphism and colloidal gold labelling. Micron 38 (5), 513–521. https://doi.org/10.1016/j.micron.2006.07.026.

Hellauer, H., Winkler, R., 1975. Denaturation of collagen fibers in NaI, NaCL and water of different pH values as studied by differential scanning calorimetric measurements. Connect. Tissue Res. 3 (4), 227–230. https://doi.org/10.3109/03008207509152182.

Hernandez-Izquierdo, V.M., Krochta, J.M., 2008. Thermoplastic processing of proteins for film formation—a review. J. Food Sci. 73 (2). https://doi.org/10.1111/j.1750-3841.2007.00636.x.

Hoque, Md S., Benjakul, S., Prodpran, T., 2011. Effects of partial hydrolysis and plasticizer content on the properties of film from cuttlefish (Sepia pharaonis) skin gelatin. Food Hydrocoll. 25 (1), 82–90. https://doi.org/10.1016/j.foodhyd.2010.05.008.

Huang, P., Li, L., Hsieh, D.-J., Chang, K.-C., 2022. Electro-optic optimization of porcine collagen through protein-amicable supercritical treatment. ACS Sustain. Chem. Eng. 10 (48), 16037–16045. https://doi.org/10.1021/acssuschemeng.2c05700.

Kikic, I., Vecchione, F., Alessi, P., Cortesi, A., Eva, F., Elvassore, N., 2003. Polymer plasticization using supercritical carbon dioxide: experiment and modeling. Ind. Eng. Chem. Res. 42 (13), 3022–3029. https://doi.org/10.1021/ie020961h.

Klüver, E., Meyer, M., 2013. Preparation, processing, and rheology of thermoplastic collagen. J. Appl. Polym. Sci. 128 (6), 4201–4211. https://doi.org/10.1002/app.38644.

Langmaier, F., Mokrejs, P., Kolomaznik, K., Mladek, M., 2008. Plasticizing collagen hydrolysate with glycerol and low-molecular weight poly(ethylene glycols). Thermochim. Acta 469 (1–2), 52–58. https://doi.org/10.1016/j.tca.2008.01.003.

Lee, M., Park, C.B., Tzoganakis, C., 1999. Measurements and modeling of PS/supercritical CO_2 solution viscosities. Polym. Eng. Sci. 39 (1), 99–109. https://doi.org/10.1002/pen.11400.

Lin, J., Pan, D., Sun, Y., Ou, C., Wang, Y., Cao, J., 2019. The modification of gelatin films: based on various cross-linking mechanism of glutaraldehyde at acidic and alkaline conditions. Food Sci. Nutr. 7 (12), 4140–4146. https://doi.org/10.1002/fsn3.1282.

Luo, Q., Hossen, M.A., Zeng, Y., Dai, J., Li, S., Qin, W., Liu, Y., 2022. Gelatin-based composite films and their application in food packaging: a review. J. Food Eng. 313, 110762. https://doi.org/10.1016/j.jfoodeng.2021.110762.

Maria Martelli, S., Moore, G., Silva Paes, S., Gandolfo, C., Laurindo, J.B., 2006. Influence of plasticizers on the water sorption isotherms and water vapor permeability of chicken feather keratin films. LWT - Food Sci. Technol. (Lebensmittel-Wissenschaft -Technol.) 39 (3), 292–301. https://doi.org/10.1016/j.lwt.2004.12.014.

Martín-de León, J., Pura, J.L., Rodríguez-Méndez, M.L., Rodríguez-Pérez, M.A., 2024. Viscoelastic property enhancement of polymethylmethacrylate molecularly confined within 3D nanostructures. Eur. Polym. J. 214, 113181. https://doi.org/10.1016/j.eurpolymj.2024.113181.

Martins, V.G., Romani, V.P., Martins, P.C., Nogueira, D., 2021. Protein-based materials for packaging applications. In: Bio-based Packaging. Wiley, pp. 27–49. https://doi.org/10.1002/9781119381228.ch2.

Martucci, J.F., Accareddu, A.E.M., Ruseckaite, R.A., 2012. Preparation and characterization of plasticized gelatin films cross-linked with low concentrations of Glutaraldehyde. J. Mater. Sci. 47 (7), 3282–3292. https://doi.org/10.1007/s10853-011-6167-3.

Martucci, J.F., Gende, L.B., Neira, L.M., Ruseckaite, R.A., 2015. Oregano and lavender essential oils as antioxidant and antimicrobial additives of biogenic gelatin films. Ind. Crop. Prod. 71, 205–213. https://doi.org/10.1016/j.indcrop.2015.03.079.

Mauri, A.N., Añón, M.C., 2006. Effect of solution pH on solubility and some structural properties of soybean protein isolate films. J. Sci. Food Agric. 86 (7), 1064–1072. https://doi.org/10.1002/jsfa.2457.

Meereboer, K.W., Misra, M., Mohanty, A.K., 2020. Review of recent advances in the biodegradability of polyhydroxyalkanoate (PHA) bioplastics and their composites. Green Chem. 22 (17), 5519–5558. https://doi.org/10.1039/D0GC01647K.

Mendes, A.C., Pedersen, G.A., 2021. Perspectives on sustainable food packaging:– is bio-based plastics a solution? Trends Food Sci. Technol. 112, 839–846. https://doi.org/10.1016/j.tifs.2021.03.049.

Meyer, M., Prade, I., Leppchen-Fröhlich, K., Felix, A., Herdegen, V., Haseneder, R., Repke, J.-U., 2015. Sterilisation of collagen materials using hydrogen peroxide doted supercritical carbon dioxide and its effects on the materials properties. J. Supercrit. Fluids 102, 32–39. https://doi.org/10.1016/j.supflu.2015.04.006.

Miles, C.A., Avery, N.C., Rodin, V.V., Bailey, A.J., 2005. The increase in denaturation temperature following cross-linking of collagen is caused by dehydration of the fibres. J. Mol. Biol. 346 (2), 551–556. https://doi.org/10.1016/j.jmb.2004.12.001.

Miles, C.A., Bailey, A.J., 1999. Thermal denaturation of collagen revisited. Proc. Ind. Acad. Sci. 111 (1), 71–80. https://doi.org/10.1007/BF02869897.

Miranda, C.S., Ferreira, M.S., Magalhães, M.T., Santos, W.J., Oliveira, J.C., Silva, J.B.A., José, N.M., 2015. Mechanical, thermal and barrier properties of starch-based films plasticized with glycerol and lignin and reinforced with cellulose nanocrystals. Mater. Today Proc. 2 (1), 63–69. https://doi.org/10.1016/j.matpr.2015.04.009.

Ochoa-Yepes, O., Di Giogio, L., Goyanes, S., Mauri, A., Famá, L., 2019. Influence of process (extrusion/thermo-compression, casting) and lentil protein content on physicochemical properties of starch films. Carbohydr. Polym. 208, 221–231. https://doi.org/10.1016/j.carbpol.2018.12.030.

Oechsle, A.M., Häupler, M., Weigel, F., Gibis, M., Kohlus, R., Weiss, J., 2016. Modulation of extruded collagen films by the addition of co-gelling proteins. J. Food Eng. 171, 164–173. https://doi.org/10.1016/j.jfoodeng.2015.10.004.

Paluch, M., Ostrowska, J., Tyński, P., Sadurski, W., Konkol, M., 2022. Structural and thermal properties of starch plasticized with glycerol/urea mixture. J. Polym. Environ. 30 (2), 728–740. https://doi.org/10.1007/s10924-021-02235-x.

Ramos, M., Valdés, A., Beltrán, A., Garrigós, M., 2016. Gelatin-based films and coatings for food packaging applications. Coatings 6 (4), 41. https://doi.org/10.3390/coatings6040041.

Riaz, A., Lagnika, C., Abdin, M., Hashim, M.M., Ahmed, W., 2020. Preparation and characterization of chitosan/gelatin-based active food packaging films containing apple peel nanoparticles. J. Polym. Environ. 28 (2), 411–420. https://doi.org/10.1007/s10924-019-01619-4.

Seo, H.J., Seo, Y.H., Park, S.U., Lee, H.J., Lee, M.R., Park, J.H., Cho, W.Y., Lee, P.C., Lee, B.Y., 2024. Glycerol-derived organic carbonates: environmentally friendly plasticizers for PLA. RSC Adv. 14 (7), 4702–4716. https://doi.org/10.1039/D3RA08922C.

Shankar, S., Wang, L.-F., Rhim, J.-W., 2019. Effect of melanin nanoparticles on the mechanical, water vapor barrier, and antioxidant properties of gelatin-based films for food packaging application. Food Packag. Shelf Life 21, 100363. https://doi.org/10.1016/j.fpsl.2019.100363.

Sid, S., Mor, R.S., Kishore, A., Sharanagat, V.S., 2021. Bio-sourced polymers as alternatives to conventional food packaging materials: a review. Trends Food Sci. Technol. 115, 87–104. https://doi.org/10.1016/j.tifs.2021.06.026.

Sionkowska, A., 2004. Molecular interactions in collagen and chitosan blends. Biomaterials 25 (5), 795–801. https://doi.org/10.1016/S0142-9612(03)00595-7.

Sothornvit, R., Krochta, J.M., 2005. Plasticizers in edible films and coatings. In: Innovations in Food Packaging. Elsevier, pp. 403–433. https://doi.org/10.1016/B978-012311632-1/50055-3.

Staicu, T., Cîrcu, V., Ioniță, G., Ghica, C., Popa, V.T., Micutz, M., 2015. Analysis of bimodal thermally-induced denaturation of type I collagen extracted from calfskin. RSC Adv. 5 (48), 38391–38406. https://doi.org/10.1039/C5RA02708J.

Stejskal, N., Miranda, J.M., Martucci, J.F., Ruseckaite, R.A., Aubourg, S.P., Barros-Velázquez, J., 2020. The effect of gelatine packaging film containing a spirulina platensis protein concentrate on atlantic mackerel shelf life. Molecules 25 (14), 3209. https://doi.org/10.3390/molecules25143209.

Tang, C., Zhou, K., Zhu, Y., Zhang, W., Xie, Y., Wang, Z., Zhou, H., Yang, T., Zhang, Q., Xu, B., 2022. Collagen and its derivatives: from structure and properties to their applications in food industry. Food Hydrocoll. 131, 107748. https://doi.org/10.1016/j.foodhyd.2022.107748.

Tardy, B.L., Richardson, J.J., Greca, L.G., Guo, J., Bras, J., Rojas, O.J., 2022. Advancing bio-based materials for sustainable solutions to food packaging. Nat. Sustain. 6 (4), 360–367. https://doi.org/10.1038/s41893-022-01012-5.

Teixeira, S.C., Silva, R.R.A., de Oliveira, T.V., Stringheta, P.C., Pinto, M.R.M.R., Soares, N. de F.F., 2021. Glycerol and triethyl citrate plasticizer effects on molecular, thermal, mechanical, and barrier properties of cellulose acetate films. Food Biosci. 42, 101202. https://doi.org/10.1016/j.fbio.2021.101202.

Versino, F., Ortega, F., Monroy, Y., Rivero, S., López, O.V., García, M.A., 2023. Sustainable and bio-based food packaging: a review on past and current design innovations. Foods 12 (5), 1057. https://doi.org/10.3390/foods12051057.

Watanabe, M., Hashimoto, Y., Kimura, T., Kishida, A., 2020. Characterization of engineering plastics plasticized using supercritical CO_2. Polymers 12 (1), 134. https://doi.org/10.3390/polym12010134.

Zhang, C., Nair, S.S., Chen, H., Yan, N., Farnood, R., Li, F., 2020. Thermally stable, enhanced water barrier, high strength starch bio-composite reinforced with lignin

containing cellulose nanofibrils. Carbohydr. Polym. 230, 115626. https://doi.org/10.1016/j.carbpol.2019.115626.
Zhang, R., Liu, R., Han, J., Ren, L., Jiang, L., 2024. Protein-based packaging films in food: developments, applications, and challenges. Gels 10 (7), 418. https://doi.org/10.3390/gels10070418.
Zhang, T., Yu, Z., Ma, Y., Chiou, B.-S., Liu, F., Zhong, F., 2022. Modulating physicochemical properties of collagen films by cross-linking with glutaraldehyde at varied pH values. Food Hydrocoll. 124, 107270. https://doi.org/10.1016/j.foodhyd.2021.107270.